Cluster Organization and Pore Structure of Ion Channels Formed by Beticolin 3, a Nonpeptidic Fungal Toxin

Cyril Goudet,* Jean-Pierre Benitah,* Marie-Louise Milat,# Hervé Sentenac,* and Jean-Baptiste Thibaud*
*Laboratoire de Biochimie et Physiologie Moléculaire des Plantes, CNRS URA 2133/ENSA-M/INRA/UM2, 34060 Montpellier 1, and #Laboratoire de Phytopharmacie et Biochimie des Interactions Cellulaires, UA 692 INRA/Université de Bourgogne, BV 1540, 21034 Dijon, France

ABSTRACT Beticolin 3 (B3) belongs to a family of nonpeptidic phytotoxins produced by the fungus *Cercospora beticola*, which present a broad spectrum of cytotoxic effects. We report here that, at cytotoxic concentration (10 μM), B3 formed voltage-independent, weakly selective ion channels with multiple conductance levels in planar lipid bilayers. In symmetrical standard solutions, conductance values of the first levels were, respectively, 16 $\pm$ 1 pS, 32 $\pm$ 2 pS, and 57 $\pm$ 2 pS ($n = 4$) and so on, any conductance level being roughly twice the lower one. Whether a cluster organization of elementary channels or different channel structures underlies this particular property was addressed by investigating the ionic selectivity and the pore size corresponding to the first three conductance levels. Both selectivity and pore size were found to be almost independent of the conductance level. This indicated that multiple conductance behavior resulted from a cluster organization of "B3 elementary channels." According to the estimated pore size and analyses of x-ray diffraction of B3 microcrystals, a structural model for "B3 elementary channels" is proposed. The ability to form channels is likely to be involved in the biological activity of beticolins.

INTRODUCTION

Beticolins are non-host-specific toxins produced by the phytopathogenic fungus *Cercospora beticola*, which is responsible for the leaf spot disease on sugar beet. Beticolins form a family of nonpeptidic compounds (with 20 identified to date, named beticolin 0 to beticolin 19). They share the same polycyclic skeleton with a chlorine atom and partially hydrogenated anthraquinone and xanthone moieties (Fig. 1 *A*; see also Ducrot et al., 1994; Prangé et al., 1997, and references therein) but differ by isomeric configurations (*ortho*- or *para*-, Fig. 1 *A*) and by a variable residue (R in Fig. 1 *A*).

Beticolins are endowed with many cytotoxic effects. In plants, beticolins have been found to induce dramatic loss of solutes such as amino acids and β-cyanin from root tissues (Schlösser, 1971; Macri and Vianello, 1979). These toxins inhibit ATP-dependent H^+ transport in pea stem (Macri et al., 1983) and corn root (Blein et al., 1988). In tobacco cells, beticolins cause dissipation of transmembrane potential (Gapillout et al., 1996). In addition to their toxicity on plant plasma membrane, beticolins also exhibit an antibiotic activity (Schlösser, 1962). In vitro, beticolins display an O_2^- scavenging activity at lower concentration than do vitamin E and Tiron (Rustérucci et al., 1996). Moreover, beticolins show an antiproliferative effect on rat adrenocortical cell lines and mouse tumor adrenocortical cells by modulating a step of steroid biosynthetic pathway (Ding et al., 1996).

Induced permeabilization of cell membranes is one of the most common killing mechanisms of molecules that have cytotoxic functions. For several peptidic or nonpeptidic toxins or antibiotics, formation of multimeric pores has been suggested to be responsible for membrane permeabilization and cell lysis (e.g., alamethicin (Woolley and Wallace, 1992; Sansom, 1993), gramicidin (Woolley and Wallace, 1992), amphotericin B (Ramos et al., 1996), flammutoxin (Tomita et al., 1998), lycotoxin (Yan and Adams, 1998), yeast killer toxins (Kagan, 1983); see Bernheimer and Rudy, 1986; Ojcius and Young, 1991; Marsh, 1996; and Mirzabekov et al., 1999, for reviews). The deleterious properties of beticolins could originate from a pore-forming feature of these fungal toxins. Recently we have shown that (*ortho*-)beticolin 0 can form ion-permeable channels at cytotoxic concentration (Goudet et al., 1998). However, the generalization of the channel formation to the whole beticolin family is still to be demonstrated. Furthermore, the secondary structures of the pore remain essentially unknown, and little is known about the mechanisms underlying this pore formation.

Here we report that (*para*-)beticolin 3 (B3) (see Fig. 1 *B*) is able to form voltage-independent and weakly selective ion channels in planar lipid bilayers. These channels present different conductance levels, which are multiples of each other. To understand the structures underlying this property, we compared the ionic selectivity of the first three conductance levels in different salt media. We also compared the pore size of the first three conductance levels by studying the effect of different nonelectrolytes of various sizes on beticolin conductances and analyzing the dependence of

Received for publication 25 June 1999 and in final form 19 August 1999.

Address reprint requests to Dr. Jean-Baptiste Thibaud, Laboratoire de Biochimie et Physiologie Moléculaire des Plantes, CNRS URA 2133/ENSA-M/INRA/UM2, 2 Place Pierre Viala, 34060 Montpellier Cedex 1, France. Tel.: +33-499-612-609; Fax: +33-467-525-737; E-mail: thibaud@ensam.inra.fr.

Dr. Benitah's present address is Laboratoire de Physiopathologie Cardiovasculaire, INSERM U390, CHU Arnaud de Villeneuve, 34295 Montpellier, France.

0006-3495/99/12/3052/08 $2.00

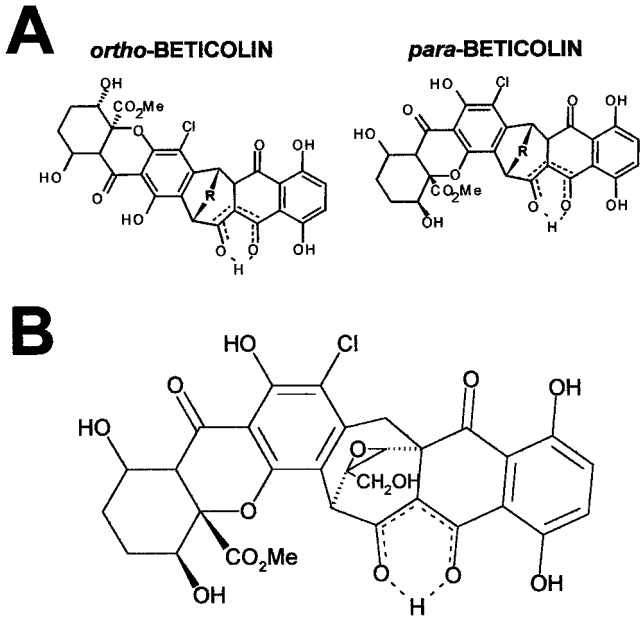

FIGURE 1 Structure of beticolins. (*A*) Structure of *ortho*- and *para*-beticolin. (*B*) B3 is a *para*-beticolin with a residue (R), which is $C_3H_4O_2$ (Ducrot et al., 1994).

single-channel conductance on the hydrodynamic radius of nonelectrolytes. Considering the high similarity of both ionic selectivity and pore radius between the different conductance levels, a cluster organization of elementary B3 channels that open and close simultaneously is likely to explain the existence of the different conductance levels. Furthermore, with our results and with data from analysis of x-ray diffraction by B3 microcrystals, we propose a model for the 3D structure of elementary ion-conducting channel(s) formed by B3 cytotoxin.

MATERIALS AND METHODS

Planar lipid bilayer

Planar bilayers were formed by painting a solution of synthetic 1-palmitoyl-2-oleoyl-phosphatidylethanolamine (POPE) and 1-palmitoyl-2-oleoyl-phosphatidylcholine (POPC) (Avanti Polar Lipids, Birmingham, AL), in a 1:1 molar ratio, dissolved in *n*-decane (10 mg·ml^{-1}; Sigma) across a 0.2-mm-diameter hole made in polyvinylidenedifluoride septum separating two chambers of 2 ml (defined as *cis* and *trans*) (Mueller et al., 1962).

Currents through the bilayer were recorded with an Axopatch 200B (Axon Instruments, Foster City, CA) patch-clamp amplifier. *Trans* and *cis* chamber solutions were connected (through 3 M KCl/AgCl/Ag half-cells) to headstage and signal-ground inputs of the amplifier, respectively. Potential values were thus defined as *trans* chamber minus *cis* chamber voltage. Membrane formation was verified by monitoring membrane capacitance and resistance. Bilayers readily formed with a capacitance of 100–150 pF. For a period of at least 30 min before toxin addition, those membranes were stables and, in standard solution, had a conductance of less than 10 pS at voltages in the ±100 mV range. Recordings were sampled at 2 kHz and filtered at 50 Hz for further analysis using pClamp 6 (Axon instruments) and Origin 4.0 (Microcal Software, Northampton, MA) softwares.

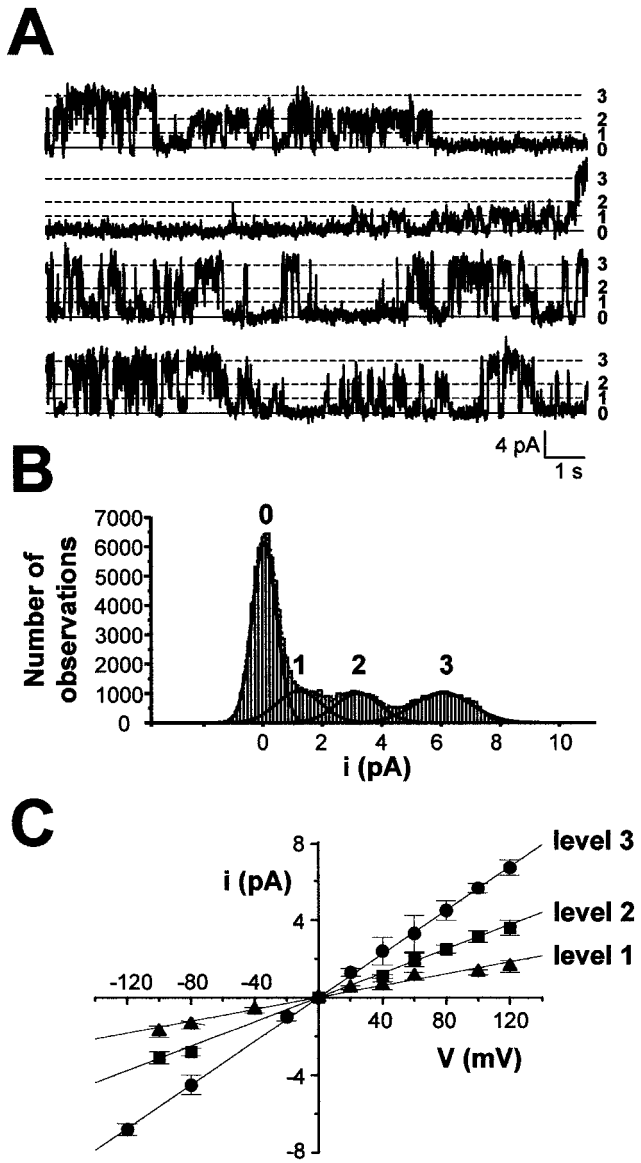

FIGURE 2 Beticolin 3 currents of different amplitudes through planar lipid bilayers. (*A*) Representative trace of channel activity recorded at +100 mV in standard symmetrical solutions after the addition of 10 μM B3 toxin to the *cis* solution. Experiments have been made using synthetic POPE/POPC lipid bilayers. Both *cis* and *trans* standard solutions contained 200 mM KCl, 0.88 mM $MgCl_2$, 1 mM EDTA, and 10 mM HEPES-KOH (pH 7.4). The free Mg^{2+} concentration was estimated to be 10 μM. Data were recorded at 2 kHz and filtered at 50 Hz. The current of the closed (0) state is indicated by the solid line. The dashed lines figure the three different discrete current levels (marked by *1, 2,* and *3,* derived from analysis of the histogram shown in *B*). (*B*) Frequency histogram of current amplitude (data from *A*) and multi-Gaussian fit. (*C*) Mean current-voltage relationships for the three open states (▲, level 1; ■, level 2; ●, level 3) of B3 channels (n = 4). Solid lines are linear fits, of which the slope corresponds to the following conductance values: 16 ± 1 pS, 32 ± 2 pS, and 57 ± 2 pS, respectively, for levels 1, 2, and 3.

Chemicals

The standard solution contained 200 mM KCl, 0.88 mM $MgCl_2$, 1 mM EDTA, and 10 mM HEPES-KOH (pH 7.4). The free Mg^{2+} concentration is estimated to be 10 μM. In standard experiments, both the *cis* and *trans* chambers contained the standard solution.

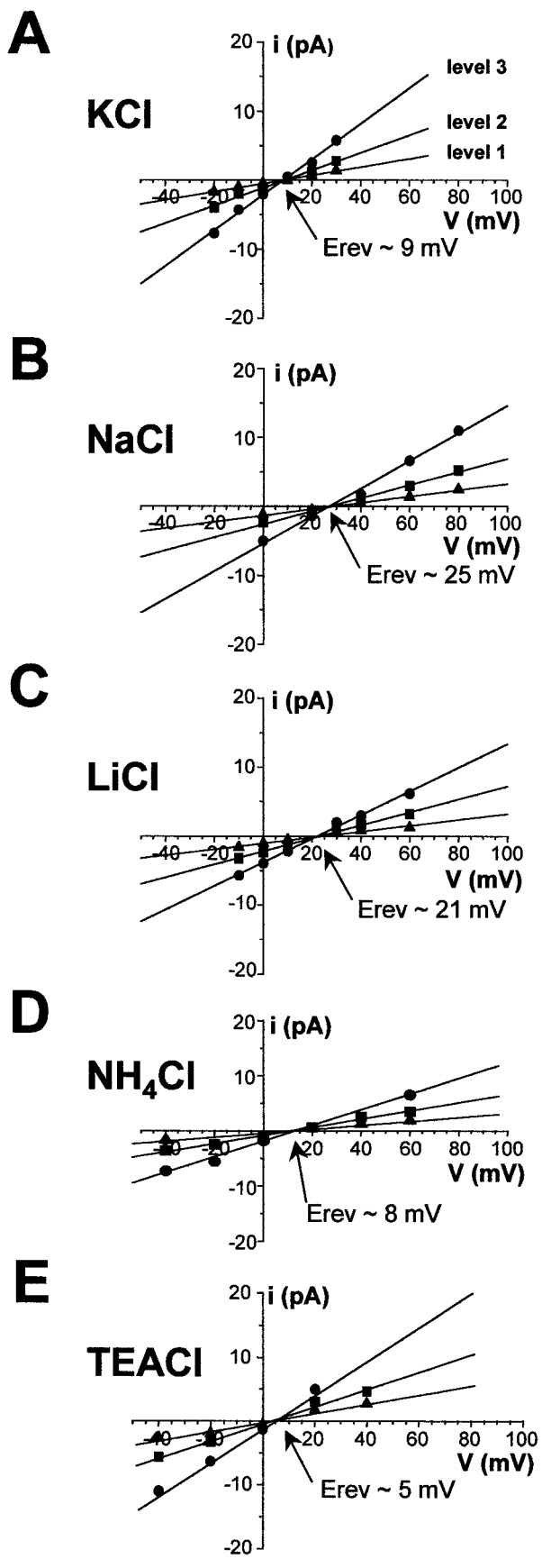

FIGURE 3 Similar reverse potential of the first three amplitude levels of B3 channels in different asymmetrical media. Current-voltage relationships of the multiple B3 conductance levels (▲, level 1; ■, level 2; ●, level 3) in different asymmetrical media. The *trans* medium contained 100 mM XCl (where X = K in *A*, Na in B, Li in *C*, NH_4 in *D*, and TEA in E), whereas the *cis* medium contained 500 mM XCl. Both *cis* and *trans* medium also contained 0.88 mM $MgCl_2$, 1 mM EDTA, and 10 mM HEPES-KOH (pH 7.4). The free Mg^{2+} concentration was estimated to be 10 μM. In each condition, reverse potentials of the different amplitude levels were very close. The data shown are representative of at least three experiments.

To determine the channel ionic selectivity, the reversal potential was measured in asymmetrical solutions of a fivefold XCl concentration gradient (500 mM/100 mM XCl, *cis*/*trans*, with X = K, Na, Li, NH_4, or tetraethylammonium, TEA), substituting KCl in the standard solutions. The cation/anion permeability ratio was then calculated using the Goldman-Hodgkin-Katz equation (Hille, 1992).

Beticolin 3 was extracted from *C. beticola* mycelium (strain CM) and purified as previously described (Milat et al., 1993). B3 was added in the stirred *cis* solution at a concentration of 10 μM.

Pore size determination

Pore size determination was performed using nonelectrolyte (NE) molecules of different hydrodynamic sizes (Carneiro et al., 1997; Krasilnikov et al., 1997, 1998; Kaulin et al., 1998; Krasilnikov et al., 1998). Briefly, 20% (w/v) of a specified NE was added to the standard solution in both chambers. The following NEs were used: glucose, fructose, sorbitol (Sigma), and different polyethylene glycols (PEGs): 300, 400, 600, 1000, 3000, and 8000 (Fluka). The conductivities of these solutions were measured with a conductimeter (CD16; Tacusel Electronique, Villeurbanne, France). Then the maximum pore radius was determined by measuring B3 single-channel conductances (γ) in the different solutions. As described by Krasilnikov et al. (1997), the filling parameter (η) was calculated as follows:

$$\eta = [(\gamma_0 - \gamma_s)/\gamma_s]/[(\chi_0 - \chi_s)/\chi_s] \quad (1)$$

Where γ_s and γ_0 are the single-channel conductances, respectively, in the presence or absence of a given NE and χ_s and χ_0 are the conductivities of the solutions. The relationship between η and the hydrodynamic radius of the NE allowed the determination of the maximum pore radius from the intercept between the decreasing linear portion of the relation (where NE is able to enter the channel and η decreases with increasing NE radius) and the quasihorizontal portion (where NE is unable to enter the pore and η is independent of the hydrodynamic radius).

All results from different experiments are expressed as mean ± SE.

RESULTS

Multiple conductance levels of B3 channels

A few minutes after the addition of 10 μM B3 to the *cis* medium, discrete jumps in the current to multiple levels were observed. Fig. 2 *A* shows an example of a 50-s-long current record displaying different amplitude levels. The corresponding amplitude histogram is shown in Fig. 2 *B*. The envelope of this histogram could be satisfactorily fitted by a sum of four Gaussian functions (*dashed curve* in Fig. 2 *B*). The four corresponding peaks (*solid lines* in Fig. 2 *B*) are centered on the four discrete current levels that can be distinguished in the record (*four dashed lines* in Fig. 2 *A*). The left-hand peak corresponded to the leak current (<1 pA) and was taken as the baseline. The other peaks were

TABLE 1 Ionic permeability coefficient ratios of the first three conductance levels of B3 channels in asymmetrical solutions

Conductance level	Permeability coefficient ratios P_X/P_{Cl} for the following X cations:				
	Na^+ ($n = 6$)	Li^+ ($n = 4$)	K^+ ($n = 4$)	NH_4^+ ($n = 3$)	TEA^+ ($n = 3$)
1	5.3 ± 0.9	3.9 ± 1.0	1.8 ± 0.1	1.7 ± 0.2	1.2 ± 0.1
2	5.4 ± 0.7	3.8 ± 0.8	1.8 ± 0.1	1.6 ± 0.2	1.2 ± 0.1
3	5.6 ± 1.1	3.8 ± 0.6	1.9 ± 0.2	1.5 ± 0.1	1.2 ± 0.1

Current reversal potentials determined from plots like those presented in Fig. 3 were used to calculate P_X/P_{Cl} permeability ratios according to the Goldman-Hodgkin-Katz equation. Values are mean ± SE of n experiments.

centered on the following values (relative to the baseline): 1.3, 3.1, and 6.0 pA (*from left to right*). In this example only four current levels could be detected. But whenever more peaks were observed in other experiments (not shown, but see Discussion), they were always centered on values in an approximately twofold geometric progression.

Current records similar to that presented in Fig. 2 *A* were measured at different voltages from −120 to +120 mV. From this we derived the current-voltage relation of the three conductance levels detected above. The three *I-V* curves were linear and crossed the origin (Fig. 2 *C*). The slope conductances were 16 ± 1, 32 ± 2, and 57 ± 2 pS ($n = 4$). The first three conductance levels elicited by B3 are referred to as γ1 to γ3. A fourth conductance level (γ4) was occasionally observed and had a conductance value of 111 ± 3 pS ($n = 3$).

Ionic selectivity of B3 current

The cation/anion selectivity of B3 channels was determined by measuring the reversal potential (E_{rev}) in a 5:1 (*cis/trans*) concentration gradient of chloride salts, KCl, NaCl, LiCl, NH_4Cl, or TEACl (Fig. 3). Under any condition, E_{rev} was approximately the same for the first three conductance levels, γ1 to γ3: the values were within 3 mV of the average given in each panel of Fig. 3. This finding clearly indicates a similar ionic selectivity for γ1 to γ3.

From the E_{rev} values obtained in asymmetrical KCl, NaCl, LiCl, NH_4Cl, or TEACl solutions, permeability ratios (P_X/P_{Cl}) were derived (Table 1), and the following selectivity sequence was deduced: $Na^+ > Li^+ > K^+ > NH_4^+ > TEA^+ > Cl^-$.

Pore size determination

The maximum pore size was determined by analyzing B3-elicited conductances in solutions containing 20% (w/v) NEs with different hydrodynamic radii. These compounds decreased the electric conductivity of the solution (Table 2) and modified the γ values elicited by B3. When plotted against the NE hydrodynamic radius (r), γ1, γ2, and γ3 displayed a similar pattern of variation (Fig. 4). NEs with r smaller than 7 Å affected γ values, while those with r

TABLE 2 Conductivity of ionic standard solutions containing 20% (w/v) of the different nonelectrolytes used in pore size determination experiments

NE	Hydrodynamic radius (Å)	Conductivity (mS)
None	0	20
Glucose	3.7	12
Sorbitol	3.9	12
Sucrose	4.7	12
PEG 300	6	10.4
PEG 400	7	10.1
PEG 600	8	10.1
PEG 1000	9.4	10.1
PEG 3000	14.4	10
PEG 8000	30.5	9.8

Values of the NE hydrodynamic radius were taken from Carneiro et al. (1997) and Krasilnikov et al. (1998).

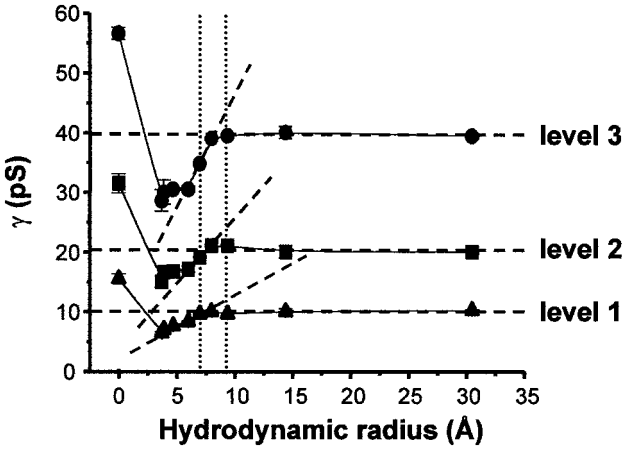

FIGURE 4 Similar dependence of the first three conductance levels of B3 channels on the hydrodynamic radii of nonelectrolytes (NEs) added to both sides of the bilayer. Chord conductance of single channels (γ) versus NE radius (▲, level 1; ■, level 2; ●, level 3). Single-channel events were recorded at +100 mV in standard symmetrical solutions (as indicated in Fig. 2) containing 20% (w/v) of a test NE. Average conductance was calculated from more than 100 current transitions registered in each experimental condition, using Ohm's law. The hydrodynamic radii of NE were taken from Table 2. For the three different conductance levels a similar relation was observed. The horizontal dashed lines were plotted between experimental points corresponding to NE's radius in the 8–30.5-Å range, where γ did not vary. The two vertical dotted lines indicated the minimum (~7 Å) and maximum (~8 Å) values of the apparent pore size of B3 channels.

greater than 8 Å did not (*horizontal dashed lines* in Fig. 4). These data suggest that any conductance level involved a similar pore radius in the range of 7–8 Å (marked by *vertical dotted lines*).

Consideration of the filling parameter η (calculated according to Eq. 1) has been shown to allow more acute determination of the pore size (Krasilnikov et al. 1998). Consistent with our above findings, the dependence of η on r was similar for $\gamma 1$, $\gamma 2$, and $\gamma 3$ (Fig. 5). As described by Krasilnikov et al. (1998), an estimate for the pore radius was obtained from the intercept between the decreasing linear and the quasihorizontal portions of the relationship. Following this method, the estimated pore radius was close to 7.5 Å for all three conductance levels considered (Fig. 5).

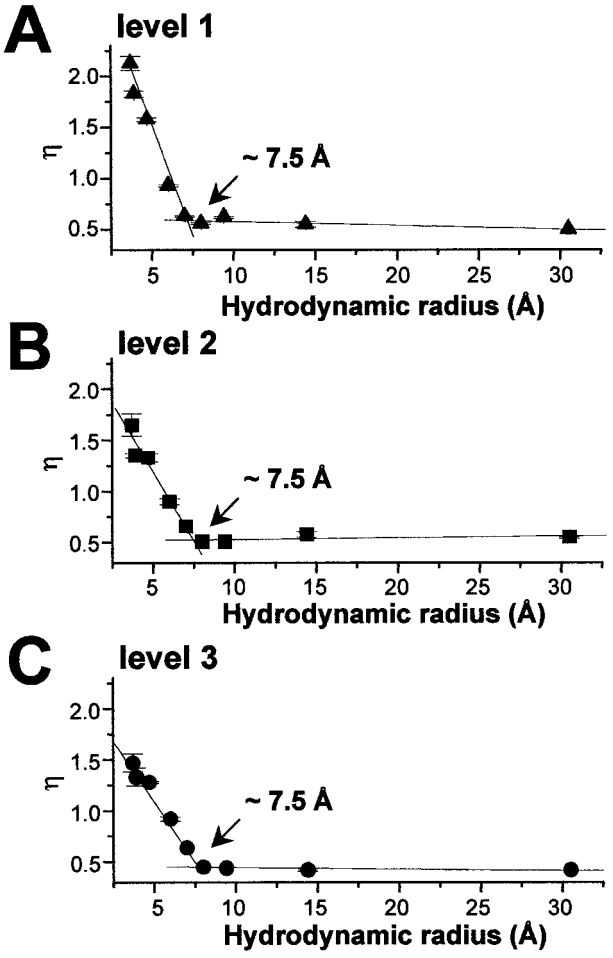

FIGURE 5 Similar estimated pore size of the first three conductance levels of B3 channels. The filling parameter η derived from the first three conductance levels of B3 channels (*from top to bottom*: (*A*) ▲, level 1; (*B*) ■, level 2; (*C*) ●, level 3) are plotted against the hydrodynamic radii of nonelectrolytes (NEs) added to both sides of the bilayer. The parameter η was calculated using Eq. 1 (see in Experimental Procedures) according to the conductance values from Fig. 4. In the three panels, linear regressions on data corresponding to NE's radius in the 8–30.5-Å range resulted in a quasihorizontal line. Other sloped linear regressions were made on data corresponding to NE's radius in the 3.7–7-Å range. The intersection between the former and latter linear regressions gave an estimate of the maximum pore radius of B3 channels. This estimate was 7.5 Å regardless of the considered conductance level.

DISCUSSION

Ability to form channels in biomembranes: a structural scheme common to the whole beticolin family?

We have previously shown that B0 is able to form channels in the plasma membrane of plant protoplasts or *Xenopus laevis* oocytes, as well as in artificial bilayers (Goudet et al., 1998). B3 differs from B0 by an isomerization (*para* versus *ortho*) and the R residue (see Fig. 1 *A*), which is $C_3H_4O_2$ for B3 and C_3H_4 for B0. With the present observation that B3 is also able to form channels in bilayers, it might be proposed that this property is a general feature of the whole beticolin family regardless of isomerization and R-substitution type.

The free Mg^{2+} and B3 concentrations used in the current experiments were chosen based on previous B0 studies. Macroscopic currents could be recorded in the presence of high Mg^{2+} concentration (data not shown). The low used free concentration of Mg^{2+} (10 μM) made it possible to record reproducibly "single-channel" rather than macroscopic B3 currents and to observe the multiple conductance behavior of B3 channels.

X-ray diffraction of B3 microcrystals allowed the determination of the 3D structure of the toxin molecule, the length of which is ~17 Å (Fig. 1) (Prangé et al., 1997). Therefore, a multimeric assembly is likely to be necessary to form a pore across a 30-Å-thick bilayer (Aidley and Stanfield, 1996). Beticolins can assemble themselves into dimeric structures in the absence of Mg^{2+} (Prangé et al., 1997). However, in the presence of Mg^{2+}, a more stable, electrically neutral dimer assembles, which is made of two beticolin molecules and two Mg^{2+} ions (Gomès et al., 1996). Interestingly, this association with Mg^{2+} strongly increases the partitioning of the toxin into the hydrophobic phase (Mikes et al., 1994). The 3D structure of the complex made of two B1 molecules and two Mg^{2+} ions was elucidated previously (Jalal et al., 1992). B1 is a *para*-beticolin, very similar to B3: the only difference is a CH_3 in B1 that is replaced by a CH_2OH in B3 (within the R-residue). Comparison of the 3D structures proposed for any of these molecules shows that this substitution has a poor effect on the whole backbone shape (Prangé et al., 1997). Therefore the structural scheme demonstrated by Jalal et al. (1992) for the $(B1\text{-}Mg)_2$ complex can be extrapolated to the $(B3\text{-}Mg)_2$ complex. The former complex is shaped like a slightly twisted but open rectangular (~5 × 10 Å) cage (Jalal et al., 1992). We propose, as illustrated in Fig. 6, that the $(B3\text{-}Mg)_2$ complex has a similar design. This $(B3\text{-}Mg)_2$ complex would be the basic element of the channels formed by B3. One can imagine that the stacking of two or three such elements would constitute a tubular structure long enough to cross a bilayer and therefore to allow the transmembrane movement of ions within itself. According to our current records, the first conductance level ($\gamma 1$) may correspond to such a structure. According to data in Figs. 4 and 5, the pore

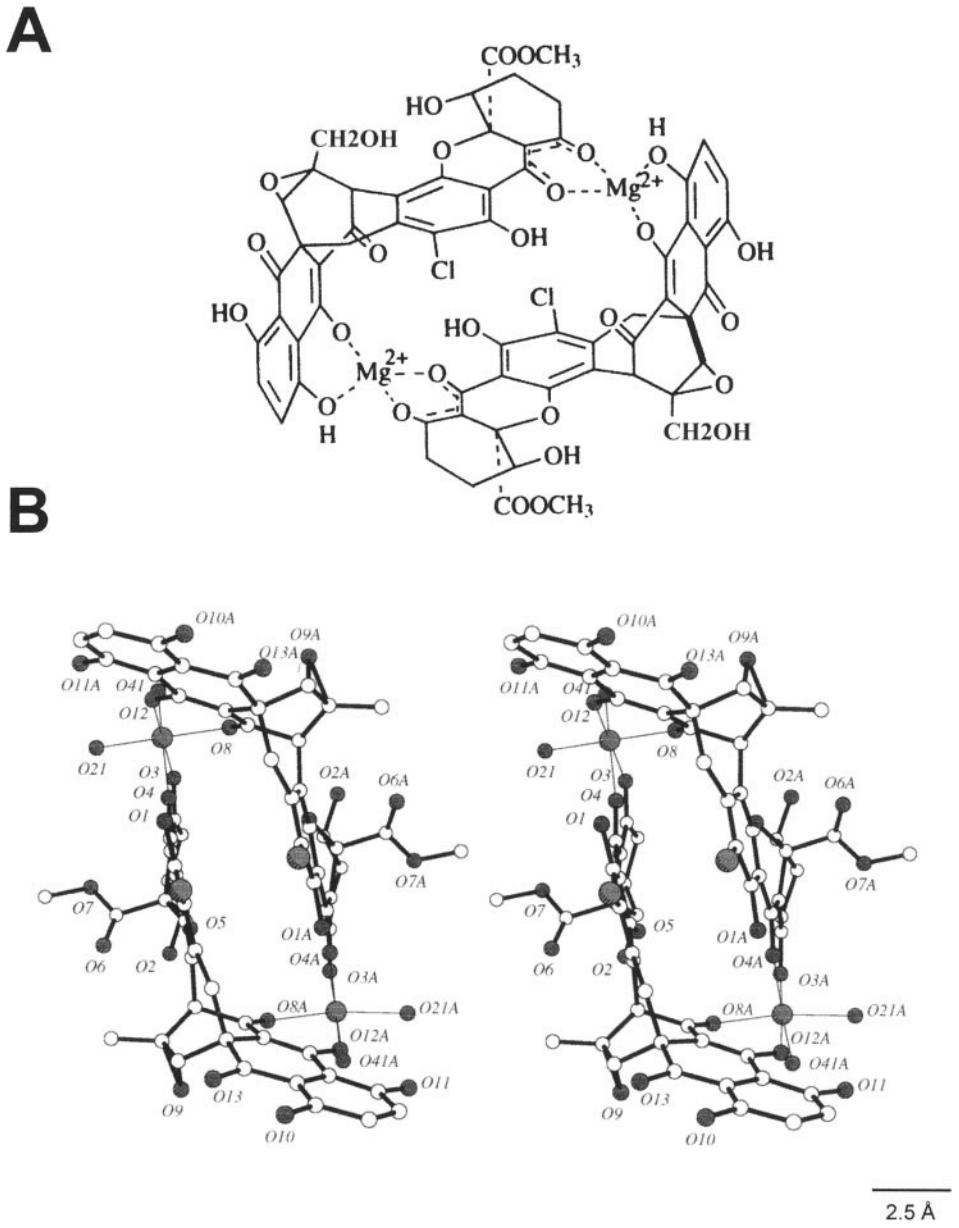

FIGURE 6 Structural model for the B3 elementary channel. (*A*) Molecular structure of a B3 dimer assembled with two Mg^{2+} (adapted from Jalal et al., 1992). (*B*) Stereo view of a B3-Mg^{2+} dimer deduced from the study of x-ray diffraction by B3 microcrystals (Prangé et al. 1997). This complex is a twisted rectangular box, the central lumen of which is assumed to make the pathway for ions (along a vertical axis perpendicular to the picture). The section of the lumen would be 10 × 5 Å (see scale bar), and three (or four) stacked dimers may form a pathway long enough (30 or 40 Å) to cross the bilayer.

radius would be 7.5 Å. This value, derived from effects of NEs, is a maximum estimate of the actual pore size. Furthermore, it is likely that the pore size is smaller for a B3 channel being part of a crystal (Fig. 6 *B*) than for a B3 channel freely "floating" in a lipid bilayer (data in Figs. 4 and 5). Therefore, there is no contradiction between our data and the above discussed structural model.

Similar ionic selectivity and pore size of multiple conductance levels of B3 channels: probable cluster organization of B3 channels

Incorporation of B3 into planar lipid bilayers resulted in single-channel events displaying multiple amplitudes, with most of the events (~80%) occurring from the baseline (Fig. 2). This suggests that multiple current amplitudes were not due to superimposed openings of several B3 channels, but rather supports the hypothesis that B3 is able to form channels endowed with multiple conductance levels. Two hypotheses can be considered regarding the type of channel structures that could underlie such behavior: 1) a cluster organization of elementary channels that open and close simultaneously or 2) different channel structures. For example, these structural organizations have been proposed for channels formed, respectively, by syringomycin E (Feigin et al., 1996; Kaulin et al., 1998) and by alamethicin (Meves and Nagy, 1989; Woolley and Wallace, 1992; Bezrukov and Vodyanoy, 1993; Vodyanoy et al., 1993).

Regarding B3 channels, the fact that the first three conductance levels are multiples of each other is a strong support for the cluster hypothesis. As shown in Fig. 6, some free phenol groups, turned out from the structure, are

present in the $(B3\text{-}Mg)_2$ complex and could favor the proposed clustering process, which would involve a decrease in the surface polarity of the assembly. Further support for the cluster model was gained from ionic selectivity and pore size studies.

Reversal potentials were determined in asymmetrical *cis*/*trans* solutions of KCl, NaCl, LiCl, NH_4Cl, or TEACl. The permeability ratios derived from the data, using the Goldman-Hodgkin-Katz equation, indicated that B3 channels were poorly selective, as previously reported for B0 channels (Goudet et al., 1998). This poor ionic selectivity is in agreement with the pore size value discussed above. However, in any ionic condition tested, reversal potential values were very close to each other for the first three levels of conductance (Fig. 3 and Table 1). This finding indicates that channel structures underlying the first three conductance levels have similar ionic selectivities.

It is widely accepted that the ionic selectivity of ion channels results from interactions between permeating ions and the pore wall (Imoto, 1993). Therefore, similar ionic selectivities for the different conductance levels of B3 channels suggest similar pore structure and size, as they would be within clusters. Indeed, NEs of different hydrodynamic radii similarly influenced the first three conductance levels of B3 channels (Figs. 4 and 5). Therefore, the pore size estimate that could be deduced from the data was the same for any of $\gamma 1$ to $\gamma 3$. This finding strongly supports the hypothesis of a cluster organization of B3 channels.

As discussed above, elementary B3 channels (corresponding to $\gamma 1$) would have a (maximum) 7.5-Å pore radius and a 16-pS single-channel conductance (in 200 mM KCl). Clusters would be made of pairs or tetrads of such elementary channels ($\gamma 2$ being twice $\gamma 1$, and $\gamma 3$ twice $\gamma 2$).

The elementary conductance of B3 channels is in the same range as that of ion channels formed by toxins with similar pore size: e.g., syringomycin E (~30 pS in 0.1 M NaCl/20 Å pore diameter) (Kaulin et al. 1998), α-hemolysin (~40 pS in 0.3 M KCl/~14 Å pore diameter) (Menestrina 1986; Song et al. 1996), and colicin Ia (~90 pS in 1.77 M KCl/~14 Å pore diameter) (Krasilnikov et al. 1998).

Biological significance

In the present study, B3 is found to form poorly selective ion channels. Moreover, the pore size of B3 channels (r = 7.5 Å) is such that biological solutes (e.g., glucose and sucrose, Figs. 4 and 5) are able to permeate through these channels. These findings could be consistent with previous data indicating that, in plant cells, beticolins induced a loss of electrolytes, amino acids, and betacyanine (Macri and Vianello, 1979) and depolarized transmembrane potential (Gapillout et al., 1996). Recently, we reported that another toxin of this family, beticolin 0, is also able to form poorly selective ion channels and thereby to strongly increase the membrane conductance of plant cells, animal cells, or planar lipid bilayers (Goudet et al., 1998). As channel formation by beticolin 0 seems strictly dependent on free Mg^{2+} availability, macroscopic currents can be obtained by increasing either beticolin or Mg^{2+} concentration and suppressed by, e.g., catching Mg^{2+} with an appropriate EDTA concentration (Goudet et al., 1998). Whether a low or a macroscopic conductance is induced by beticolin under physiological conditions is still unknown. Mg^{2+} concentration, which is much higher in vivo than in our conditions (10 μM), may make macroscopic beticolin conductance possible. On the other hand, it reasonably could be assumed that the beticolin concentration is much lower in vivo than in our experiments (10 μM) and therefore may limit the number of channels formed. In vivo, the channel-forming feature of beticolins may result in the collapse of ionic and electrical gradients. The ability to form channels, therefore, is likely to be involved in the biological activity of beticolins, as hypothesized for syringomycin, a necrosis-inducing lipopeptide toxin secreted by the phytopathogenic bacteria *Pseudomonas syringae* (Hutchison et al., 1995).

We are grateful to Dr. M. Tester for his helpful suggestions and critical reading of the manuscript. We acknowledge with thanks the expertise of Prof. T. Prangé in designing Fig. 6 as well as his insightful comments on the work.

This work was supported by grants from the Institut National de la Recherche Agronomique and the Conseil Régional de Bourgogne.

REFERENCES

Aidley, D. J., and P. R. Stanfield. 1996. Ion Channels: Molecules in Action. Cambridge University Press, Cambridge and New York.

Bernheimer, A. W., and B. Rudy. 1986. Interactions between membranes and cytolytic peptides. *Biochim. Biophys. Acta.* 864:123–141.

Bezrukov, S. M., and I. Vodyanoy. 1993. Probing alamethicin channels with water-soluble polymers. Effect on conductance of channel states. *Biophys. J.* 64:16–25.

Blein, J.-P., I. Bourdil, M. Rossignol, and R. Scalla. 1988. *Cercospora beticola* toxin inhibits vanadate-sensitive H^+ transport in corn root membrane vesicles. *Plant Physiol.* 88:429–434.

Carneiro, C. M., O. V. Krasilnikov, L. N. Yuldasheva, A. C. Campos de Carvalho, and R. A. Nogueira. 1997. Is the mammalian porin channel, VDAC, a perfect cylinder in the high conductance state? *FEBS Lett.* 416:187–189.

Ding, G., G. Maume, M. L. Milat, C. Humbert, J. P. Blein, and B. F. Maume. 1996. Inhibition of cellular growth and steroid 11 beta-hydroxylation in ras- transformed adrenocortical cells by the fungal toxins beticolins. *Cell Biol. Int.* 20:523–30.

Ducrot, P.-H., M.-L. Milat, J.-P. Blein, and J.-Y. Lallemand. 1994. The yellow toxins produced by *Cercospora beticola*. Revised structures of beticolin 1 and beticolin 3. *J. Chem. Soc. Chem. Commun.* 2215–2216.

Feigin, A. M., J. Y. Takemoto, R. Wangspa, J. H. Teeter, and J. G. Brand. 1996. Properties of voltage-gated ion channels formed by syringomycin E in planar lipid bilayers. *J. Membr. Biol.* 149:41–47.

Gapillout, I., V. Mikes, M.-L. Milat, F. Simon-Plas, A. Pugin, and J.-P. Blein. 1996. *Cercospora beticola* toxins. Use of fluorescent cyanine dye to study the effects on tobacco cell suspensions. *Phytochemistry.* 43: 387–392.

Gomès, E., R. Gordon-Weeks, F. Simon-Plas, A. Pugin, M. L. Milat, R. A. Leigh, and J. P. Blein. 1996. *Cercospora beticola* toxins. Part XVII. The role of the beticolin/Mg^{2+} complexes in their biological activity. Study of plasma membrane H(+)-ATPase, vacuolar H(+)-PPase, alkaline and acid phosphatases. *Biochim. Biophys. Acta.* 1285:38–46.

Goudet, C., A.-A. Véry, M.-L. Milat, M. Ildefonse, J.-B. Thibaud, H. Sentenac, and J.-P. Blein. 1998. Magnesium ions promote assembly of channel-like structures from beticolin 0, a non-peptide fungal toxin purified from *Cercospora beticola*. *Plant J.* 14:359–364.

Hille, B. 1992. Ionic Channels of Excitable Membranes. Sinauer Associates, Sunderland, MA.

Hutchison, M. L., M. A. Tester, and D. C. Gross. 1995. Role of biosurfactant and ion channel-forming activities of syringomycin in transmembrane ion flux: a model for the mechanism of action in the plant-pathogen interaction. *Mol. Plant Microbe Interact.* 8:610–20.

Imoto, K. 1993. Ion channels: molecular basis of ion selectivity. *FEBS Lett.* 325:100–103.

Jalal, M. A. F., M. B. Hossain, D. J. Robeson, and D. van der Helm. 1992. *Cercospora beticola* phytotoxins: cebetins that are photoactive, Mg^{2+}-binding, chlorinated anthraquinone-xanthone conjugates. *J. Am. Chem. Soc.* 114:5967–5971.

Kagan, B. L. 1983. Mode of action of yeast killer toxins: channel formation in lipid bilayer membranes. *Nature.* 302:709–711.

Kaulin, Y. A., L. V. Schagina, S. M. Bezrukov, V. V. Malev, A. M. Feigin, J. Y. Takemoto, J. H. Teeter, and J. G. Brand. 1998. Cluster organization of ion channels formed by the antibiotic syringomycin E in bilayer lipid membranes. *Biophys. J.* 74:2918–2925.

Krasilnikov, O. V., J. B. Da Cruz, L. N. Yuldasheva, W. A. Varanda, and R. A. Nogueira. 1998. A novel approach to study the geometry of the water lumen of ion channels: colicin Ia channels in planar lipid bilayers. *J. Membr. Biol.* 161:83–92.

Krasilnikov, O. V., L. N. Yuldasheva, P. G. Merzlyak, M. F. Capistrano, and R. A. Nogueira. 1997. The hinge portion of the *S. aureus* alpha-toxin crosses the lipid bilayer and is part of the trans-mouth of the channel. *Biochim. Biophys. Acta.* 1329:51–60.

Macri, F., P. Dell' Antone, and A. Vianello. 1983. ATP-dependent proton uptake inhibited by *Cercospora beticola* toxin in pea stem microsomal vesicle. *Plant Cell Environ.* 6:555–558.

Macri, F., and A. Vianello. 1979. Inhibition of K^+ uptake, H^+ extrusion and K^+ activated ATPase, and depolarization of transmembrane potential in plant tissues treated with *Cercospora beticola. Physiol. Plant Pathol.* 15:161–170.

Marsh, D. 1996. Peptide models for membrane channels. *Biochem J.* 315:345–361.

Menestrina, G. 1986. Ionic channels formed by *Staphylococcus aureus* alpha-toxin: voltage-dependent inhibition by divalent and trivalent cations. *J. Membr. Biol.* 90:177–190.

Meves, H., and K. Nagy. 1989. Multiple conductance states of the sodium channel and of other ion channels. *Biochim. Biophys. Acta.* 988:99–105.

Mikes, V., M.-L. Milat, A. Pugin, and J.-P. Blein. 1994. *Cercospora beticola* toxins. VII. Fluorometric study of their interactions with biological membranes. *Biochim. Biophys. Acta.* 1195:124–130.

Milat, M.-L., J.-P. Blein, J. Einhorn, J.-C. Tabet, P.-H. Ducrot, and J.-Y. Lallemand. 1993. The yellow toxins produced by *Cercospora beticola*. Part II. Isolation and structure of beticolin 3 and 4. *Tetrahedron Lett.* 34:1483–1486.

Mirzabekov, T. A., A. Y. Silberstein, and B. L. Kagan. 1999. Use of planar lipid bilayer membranes for rapid screening of membrane active compounds. *Methods Enzymol.* 294:661–674.

Mueller, P., D. O. Rudin, H. T. Tien, and W. C. Wescott. 1962. Reconstitution of cell membrane structure in vitro and its transformation into an excitable system. *Nature.* 194:979–980.

Ojcius, D. M., and J. D. Young. 1991. Cytolytic pore-forming proteins and peptides: is there a common structural motif? *Trends Biochem. Sci.* 16:225–229.

Prangé, T., A. Neuman, M.-L. Milat, and J.-P. Blein. 1997. *Cercospora beticola* toxins. Part 16. X-ray diffraction analyses on microcrystals of three *p*-beticolins. *J. Chem. Soc. Perkins Trans.* 2:1819–1825.

Ramos, H., E. Valdivieso, M. Gamargo, F. Dagger, and B. E. Cohen. 1996. Amphotericin B kills unicellular leishmanias by forming aqueous pores permeable to small cations and anions. *J. Membr. Biol.* 152:65–75.

Rustérucci, C., M.-L. Milat, and J.-P. Blein. 1996. *Cercospora beticola* toxins. Determination of O_2-scavenging activity of beticolin 1. *Phytochemistry.* 42:979–983.

Sansom, M. S. 1993. Alamethicin and related peptaibols—model ion channels. *Eur. Biophys. J.* 22:105–124.

Schlösser, E. 1962. Uber eine biologisch aktive Substanz aus *Cercospora beticola. Phytopath. Z.* 44:295–312.

Schlösser, E. 1971. The *Cercospora beticola* toxin. *Phytopathol. Medit.* 10:154–158.

Song, L., M. R. Hobaugh, C. Shustak, S. Cheley, H. Bayley, and J. E. Gouaux. 1996. Structure of staphylococcal alpha-hemolysin, a heptameric transmembrane pore. *Science.* 274:1859–1866.

Tomita, T., D. Ishikawa, T. Noguchi, E. Katayama, and Y. Hashimoto. 1998. Assembly of flammutoxin, a cytolytic protein from the edible mushroom *Flammulina velutipes*, into a pore-forming ring-shaped oligomer on the target cell. *Biochem. J.* 333:129–137.

Vodyanoy, I., S. M. Bezrukov, and V. A. Parsegian. 1993. Probing alamethicin channels with water-soluble polymers. Size-modulated osmotic action. *Biophys J.* 65:2097–2105.

Woolley, G. A., and B. A. Wallace. 1992. Model ion channels: gramicidin and alamethicin. *J. Membr. Biol.* 129:109–136.

Yan, L., and M. E. Adams. 1998. Lycotoxins, antimicrobial peptides from venom of the wolf spider *Lycosa carolinensis*. *J. Biol. Chem.* 273: 2059–2066.